Cation Effects on Infrared Reflection Absorption Spectra of Cyanide Adsorbed on Pt(111) Electrode in Electrolyte Solutions

Junji Inukai, Yukiko Morioka, Youn-Geun Kim,† Shueh-Lin Yau,† and Kingo Itaya*

Department of Applied Chemistry, Faculty of Engineering, Tohoku University, Aramaki, Aoba, Sendai 980-77

†Itaya Electrochemistry Project, ERATO, JRDC, 2-1-1 Yagiyama-minami, Taihaku-ku, Sendai 982

(Received February 21, 1997)

In-situ infrared reflection absorption spectroscopy was applied to the investigation of cation effects on the C–N stretching frequency of cyanide ions on Pt(111) electrode in electrolyte solutions. Only a single absorption peak was observed at ca. 2100 cm^{-1} in solutions containing H_3O^+, Li^+, Na^+, K^+, or Cs^+. In a $KClO_4$ solution (pH = 9.5), a change in slope was observed in the peak frequency–potential curve at ca. −0.5 V vs. the saturated calomel electrode. It was concluded that in the cathodic region in the $KClO_4$ solution, H_3O^+ dominates the outer Helmholtz plane as a result of cation exchange. In alkaline solutions, the slope for the frequency shift is dependent on the cations in the order $K^+ > Na^+ > Li^+ \approx Cs^+$. In $HClO_4$, a change in slope was also observed in the peak frequency-potential curve. In a $Mg(ClO_4)_2$ solution, three peaks were observed for CN on Pt(111), indicating that factors other than the simple electrochemical Stark effect must be considered for interpreting the influence of this strongly adsorbed cation.

Characterization of the electrochemical double layer at solid electrodes has been an important issue in electrochemistry. While the vital role of the ionic double layer at electrode-solution interfaces has prompted studies by electrochemists,[1] experimental difficulties have precluded direct structural characterization of electrode surfaces until recently. Now, for determining the adlayer structures at electrode surfaces, many in-situ techniques are available: these include infrared reflection adsorption spectroscopy (IRAS),[2] scanning tunneling microscopy (STM),[3] atomic force microscopy (AFM),[4] and surface X-ray scattering.[5] Most notable is in-situ STM as well as AFM, which made it possible to determine the real-space structures of various adlayers on well-defined single crystal electrodes with atomic resolution such as those of I^-,[6—9] Br^-,[10] and other inorganic ions including CN^- [11,12] and sulfate/disulfate.[13—17] According to the electrical double-layer theory for the electrode/electrolyte interface,[18] the structural study of the above-mentioned species, which are directly bonded to the electrode surfaces, unfolds detailed information on the inner Helmholtz plane (IHP) composed of specifically adsorbed species and water molecules.

The adsorption of cations on top of the adlayers of halides and CN^- formed on Pt single crystal electrodes was intensively investigated by Hubbard and coworkers[19—21] using an ex-situ ultrahigh vacuum-electrochemical system. It was reported that cations such as, Li^+, Na^+,K^+, Cs^+, Ca^{2+}, Ba^{2+}, and La^{3+} are adsorbed on the well-defined CN adlayer on Pt(111).[20] Clear low energy electron diffraction patterns were reported for the adsorbed cations, indicating that the cations formed ordered structures on the CN-modified Pt(111). However, the in-situ structures of the anions and cations on electrode surfaces have been a long-standing problem still waiting to be solved. In order to elucidate such double-layer structures, we recently carried out an in-situ STM investigation of CN-modified Pt(111) in both acidic and alkaline solutions containing NaCN or KCN,[12] and succeeded in direct observation of the structures of the alkali metal cations located at the outer Helmholtz plane (OHP). The cations in solution and the substrate potential exerted strong influences on the STM images.[12] It was found that CN's form a well-ordered $(2\sqrt{3}\times 2\sqrt{3})R30°$ structure on Pt(111), in which six CN's are arranged so as to form a hexagon ring in the ordered pattern. In the case of K^+ in solution, the cation was observed to be adsorbed at the center of the CN-ring at potentials more positive than ca. −0.4 V vs. the saturated calomel electrode (SCE). At more negative potentials, the adsorbed K^+ is desorbed and possibly replaced by H_3O^+. On the other hand, Na^+ cations were less strongly adsorbed on the CN layer and were fewer in number, and they did not bring about any sudden structural change.

It is expected that the cations at OHP have influence on the CN's at IHP. It was predicted that the strength of the electric field is dependent on the distance of the OHP from the electrode surface:[22] the smaller the distance, the larger the electric field, exerting the larger electrochemical Stark effect. Large cations such as Cs^+ or highly hydrated cations such as Li^+ are located at a large distance away from the surface, and thus may give smaller influences on adsorbed CN. In this paper, for a Pt(111) electrode with preadsorbed CN, we carried out an IRAS study in electrolyte solutions containing different cations. The C–N stretching frequency was measured at various potentials. The K^+ cation exchange with H_3O^+ on the C–N bonding, which we previously found to

occur by using in-situ STM,[12] was examined by using IRAS. Further investigations were carried out to determine the influence of Li^+, Cs^+, H_3O^+, and Mg^{2+} at OHP on CN at IHP. In all experiments, the effects of cations were clearly observed on the C–N stretching. To explain the peak frequency shift of CO adsorbed on Pt surfaces, the backdonation of metal electrons into CO $2\pi^*$ orbitals from metal d-orbitals has been proposed.[23,24] However, in this study for CN adsorbed on Pt, an electrochemical Stark effect[22] may explain the experimental results.

Experimental

The Pt(111) crystal (6 mm in diameter) was annealed in a hydrogen-air flame, cooled in a hydrogen atmosphere, and quenched in ultrapure water.[25] The CN layer was formed by immersing the quenched Pt(111) crystal in an aqueous solution of 2 mM NaCN for 5 min (1 M = 1 mol dm^{-3}). After the CN-layer formation, this crystal was rinsed for a few minutes in solutions used for both cyclic voltammetry (CV) and IRAS measurements. This rinsing procedure thoroughly exchanges Na^+ ions with the corresponding cations in the solution with no influence on the CN layer structure.[20] STM examinations were performed in 0.1 M $KClO_4$ (pH = 9.5). The CV and IRAS measurements were carried out in solutions containing ClO_4^- or OH^- as anions. For cations, each solution contained 0.1 M of H_3O^+, Li^+, Na^+, K^+, Cs^+, or Mg^{2+}. For pH adjustment, corresponding metal hydroxides were used.

The CV's were obtained in a three-compartment glassware with solutions fully purged with pure nitrogen. The STM experiments were carried out using a NanoScope III (Digital Instruments) with a modified STM cell. The tip was a W wire electrochemically etched in a 1 M KOH bath. The W tip was partially coated with transparent nail polish to minimize the faradaic current.[12] The Fourier transform infrared spectrometer used was a Mattson PS/2 with an MCT detector cooled with liquid nitrogen. The crystal, IRAS cell, and reflection mirrors were all installed in a sealed case, which was purged with pure nitrogen during the measurements. The IRAS cell was constructed with Teflon®. A CaF_2 prism was used for the infrared transparent window attached to the cell.[26] Spectra were obtained by using the single potential alteration (or staircase) method. With the electrode held at each specific potential, 128 interferograms were collected, co-added, and then transformed into a single-beam spectrum. The reference spectrum free of adsorbed C–N stretching for each measurement was obtained at an anodic potential where the oxidative desorption of CN and the oxidation of platinum surface occurred.[27] The spectral resolution was 8 cm^{-1}.

All chemicals were of reagent grade. Water was purified by a Milli-Q system (18.3 Ω cm). The reference electrode used was either a saturated calomel electrode (SCE) or a reversible hydrogen electrode, but all potentials are quoted against SCE.

Results and Discussion

STM Observations in $KClO_4$. Figures 1(a) and 1(b) show the CV's for Pt(111) and Pt(111)–CN in 0.1 M $NaClO_4$ and $KClO_4$, respectively, at pH = 9.5. The dashed lines are the CV's for bare Pt(111), while the solid lines are those for Pt(111) with adsorbed CN. In both solutions, bare Pt(111) yielded steady, broad peaks between −0.8 and −0.4 V. The peaks around −0.1 V are reported to be due to the adsorption and desorption of anions on Pt(111).[29,30] Once the surfaces are coated with CN, the CV's clearly changed. In

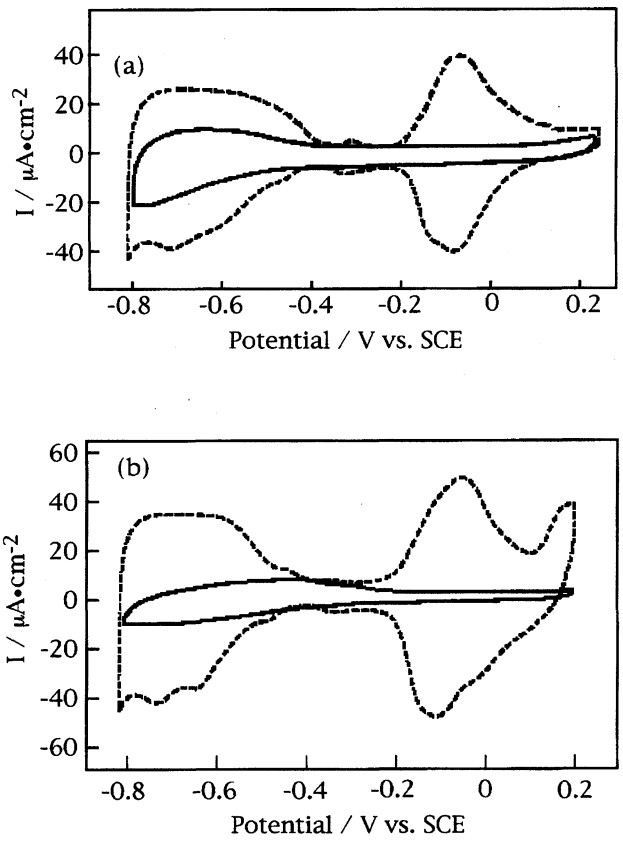

Fig. 1. Cyclic voltammograms for Pt(111) electrode in 0.1 M $NaClO_4$ (a) and $KClO_4$ (b). Solid lines: CN-coated Pt(111). Dashed lines: bare Pt(111). Scan rate = 0.05 V s^{-1}. pH = 9.5.

both solutions, the adsorption–desorption peaks observed for bare Pt(111) disappeared, the double layer region extended over the potential range between ca. −0.8 and 0.2 V. These CV's for the CN-coated Pt(111) were very steadily obtained in this potential region in many cycles.

The STM measurements were carried out on the CN-coated Pt(111) surface in 0.1 M $KClO_4$ (pH = 9.5). Figure 2(a) shows the STM image with atomic resolution obtained at a cathodic potential of −0.6 V. Well-arranged hexagonal rings are aligned in the direction rotated by 30° from the close packed directions of Pt(111), and the distance of 0.95 nm between the nearest neighbor hexagonal rings is $2\sqrt{3}$ times the lattice spacing of Pt (0.278 nm). This ordered atomic feature can be characterized as the $(2\sqrt{3}\times2\sqrt{3})$R30°-6CN structure with cyanide bound to the near-top site[12] (Fig. 3(a)). The inner space of the ring may seem to be vacant, but STM images obtained under different experimental conditions clearly resolved an additional center spot. The center spot became unclear when the tunneling current was increased. We proposed previously that either a coordinated proton (H^+) or an oxonium cation (H_3O^+) is likely located in the center of the hexagon ring.[12] After the potential was changed in the anodic direction to −0.3 V, different STM images were obtained. As shown in Fig. 2(b), bright spots appeared in the entire area with regular arrays with the spac-

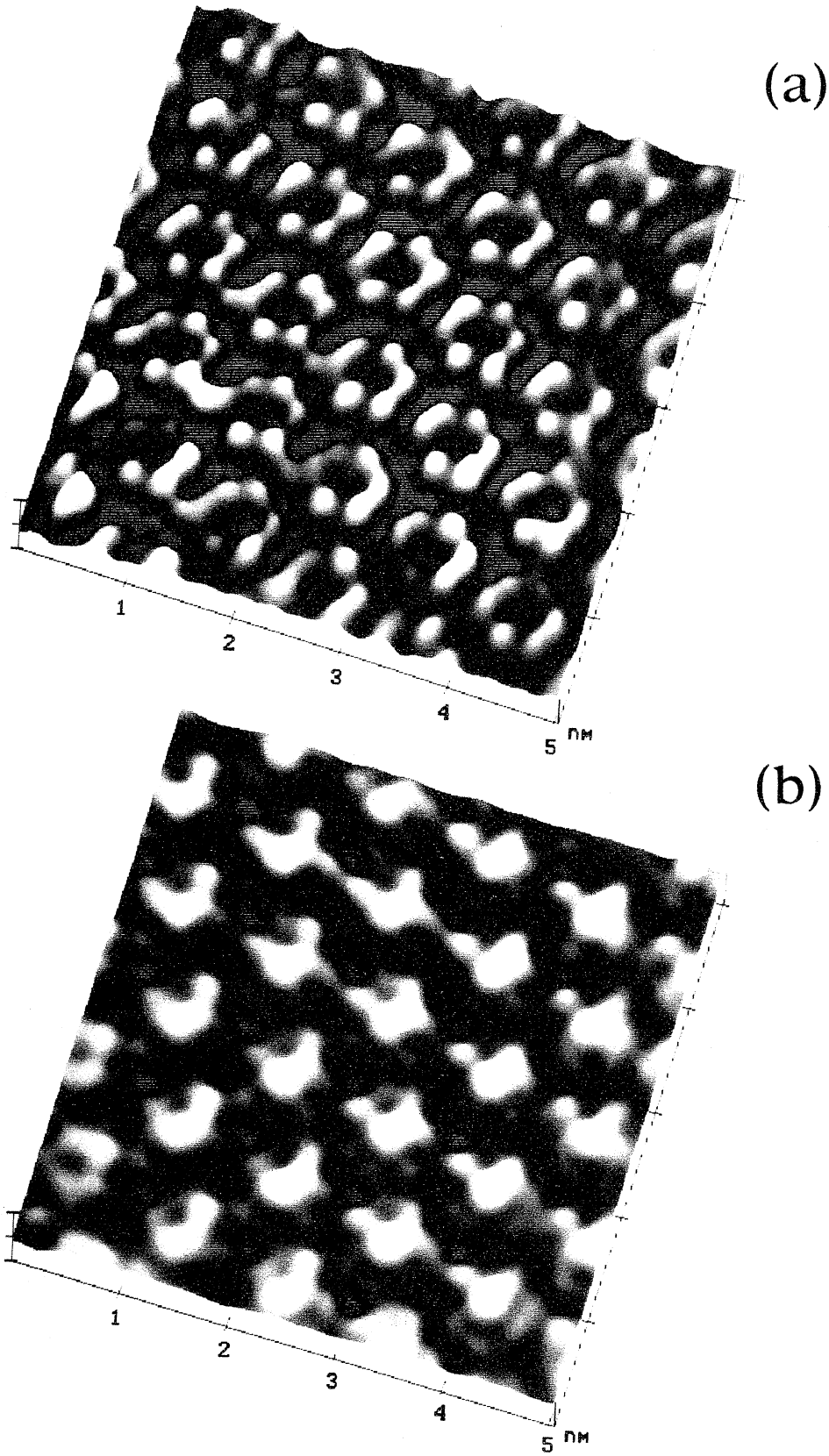

Fig. 2. STM images of Pt(111)–CN in 0.1 M $KClO_4$. pH = 9.5. Scanning area = 5 nm × 5 nm. (a): −0.6 V vs. SCE. (b): −0.3 V vs. SCE.

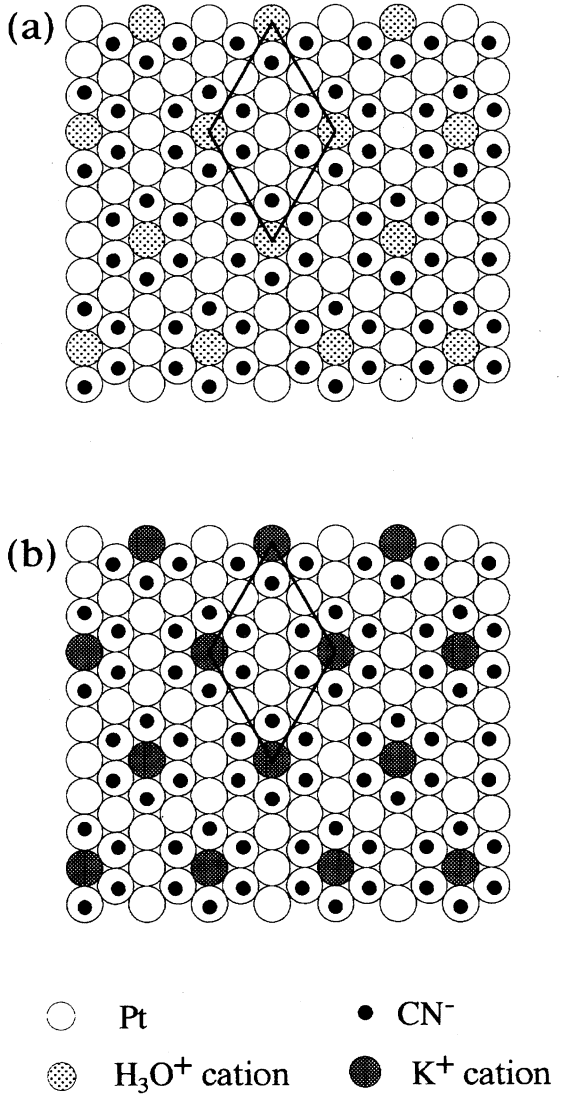

Fig. 3. Model structures of Pt(111)–CN in 0.1 M $KClO_4$ in the cathodic region (a) and in the anodic region (b).

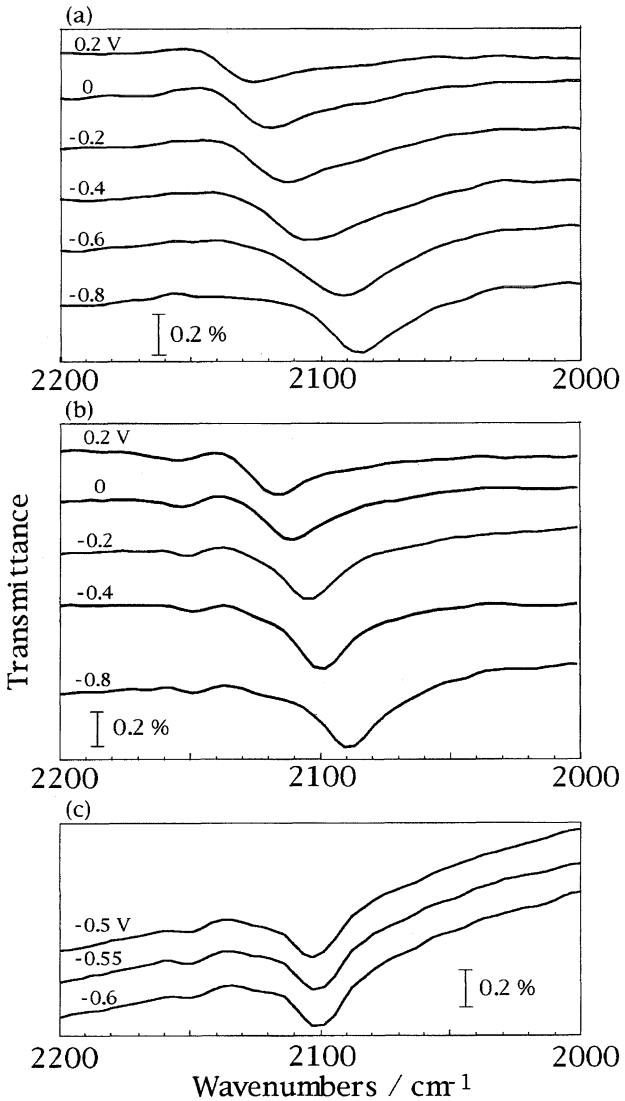

Fig. 4. Potential dependence of IR spectra of CN on Pt(111). (a): 0.1 M $NaClO_4$. (b) and (c): 0.1 M $KClO_4$. pH = 9.5. Background potential= 0.9 V vs. SCE.

ing of 0.95 nm. These bright spots have been attributed to K^+ cations located at the center of the CN-rings[12] (Fig. 3(b)). When the potential was scanned back in the cathodic direction to −0.6 V, these K^+ cations disappeared from the STM image. This cation exchange of K^+ with H_3O^+ was reexamined by using IRAS. The result will be described in the following section.

IRAS Measurements in $NaClO_4$ and $KClO_4$. IRAS measurement of CN on platinum was started by Kitamura et al.[28] in KCl solutions using polycrystalline electrodes, but the adsorption structure of CN was not clear on the disordered surfaces. Our typical set of potential dependent IRAS data for CN on Pt(111), obtained in 0.1 M $NaClO_4$ (pH=9.5), is presented in Fig. 4(a). In the potential range between −0.8 and 0.2 V, only a single peak around 2100 cm^{-1} was observed; this shifted almost linearly to higher wavenumbers with changing the potential in the anodic direction. This single peak was previously reported by Stuhlmann et al.[11] and Kim and Korzeniewski[27] for CN on Pt(111) in alkaline $NaClO_4$ solutions. Since no other peak was observed, a uniform CN-surface binding via the carbon atom was assumed, possibly in an on-top geometry.[11,27] In 0.1 M $KClO_4$ (pH = 9.5), the potential dependent single peak around 2100 cm^{-1} was similarly observed (Fig. 4(b)). Figure 4(c) also shows the spectra in $KClO_4$, but they were obtained in the narrow potential range between −0.6 and −0.5 V. In this region, the spectrum backgrounds were always tilted at a specific angle. Plots depicting the potential dependence of the C–N stretching frequencies near 2100 cm^{-1} in $NaClO_4$ and $KClO_4$ solutions (pH = 9.5) are shown in Fig. 5. For CN vibration in $NaClO_4$, the peak position at 0.2 V was observed at 2125 cm^{-1}. As the potential was scanned in the cathodic direction, the peak almost linearly shifted toward lower frequencies down to 2086 cm^{-1} at −0.8 V. In $KClO_4$, at an anodic potential of 0.2 V, the peak position coincided with that in $NaClO_4$ (2125 cm^{-1}). The peak frequency in $KClO_4$ was also lowered almost linearly in the cathodic scan until

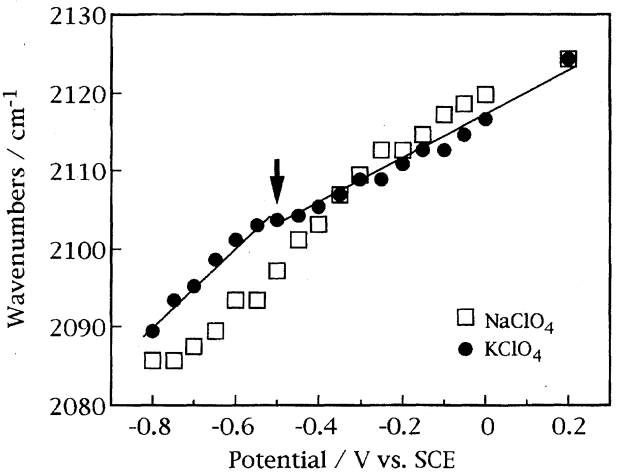

Fig. 5. Change in peak position of the stretching vibration frequency of CN on Pt(111) in 0.1 M $NaClO_4$ (open square) and $KClO_4$ (filled circle). pH=9.5. Background potential= 0.9 V vs. SCE.

−0.5 V, where the slope for the frequency shift changed. The slope became much steeper than that in the anodic region. The slope for the change in peak position with potential was 32 $cm^{-1}\,V^{-1}$ in the anodic region between 0.2 and −0.5 V, while it was 53 $cm^{-1}\,V^{-1}$ in the cathodic region between −0.5 and −0.8 V. As reported in the previous paper,[12] K^+ observed by STM at −0.35 V disappeared at −0.45 V. The change in the slope at −0.5 V observed by IRAS may correspond to this cation exchange. It is reported that the difference of cations in solution is reflected by the potential dependence of the infrared absorption bands of pseudohalide species such as CN^-. This phenomenon has been attributed principally to an electrochemical Stark effect[31,32] arising from the large electric field that exists in the double layer region. Therefore, the exchange of cations at OHP may well be expected to have influence on the potential dependence of the C–N stretching on Pt(111). The subtle potential difference of ca. 0.05 V observed between STM and IRAS results may be understood in terms of the difference in data acquisition time. As was mentioned in our previous paper, the cation exchange is a slow process.[12] At −0.45 V, the population of K^+ decreased to ca. 50% of the original quantity in 1 min after the potential was stepped from −0.35 V, and the coverage of K^+ decreased to less than 10% after 16 min in our STM data.[12] Since each IRAS was obtained in only 30 s, it may be reasonable that K^+ replacement is observed at a potential slightly different from that observed by STM. As in Fig. 4(c), the spectrum backgrounds were always tilted between −0.5 and −0.6 V. This potential region may correspond to that for the cation exchange. During the exchange of cations in this narrow potential range, the double-layer composition may have influenced the frequency dependence of the reflectivity of infrared light.

We have previously reported STM results showing that the well-ordered $(2\sqrt{3}\times2\sqrt{3})R30°$ structure underwent reconstruction to (2×2) when the potential was made more negative than −0.75 V. This potential is far more negative than that for the change in slope of the potential dependent curve for the C–N stretching peak; thus, the reconstruction is irrelevant to the origin of this bending.

IRAS Measurements in LiOH, NaOH, KOH, and CsOH. IRAS measurements were carried out in alkaline solutions of 0.1 M LiOH, NaOH, KOH, and CsOH. In these solutions, the concentration of H_3O^+ is extremely small, and the cation exchange with H_3O^+ may be prohibited, as stated in the previous paper.[12] Figure 6(a) shows CV's obtained in NaOH as an example. The dashed line is a CV recorded with bare Pt(111) in NaOH, showing hydrogen adsorption–desorption peaks between −0.95 and −0.6 V and OH^- adsorption–desorption peaks between −0.4 and −0.1 V. On the CN-coated Pt(111) (solid line in Fig. 6(a)), only very small peaks for hydrogen adsorption–desorption were observed at the onset of the hydrogen evolution.

In IRAS, single peaks at ca. 2100 cm^{-1} were observed in all four solutions (0.1 M LiOH, NaOH, KOH, and CsOH) as in the former cases with $NaClO_4$ and $KClO_4$ (pH=9.5). Fig-

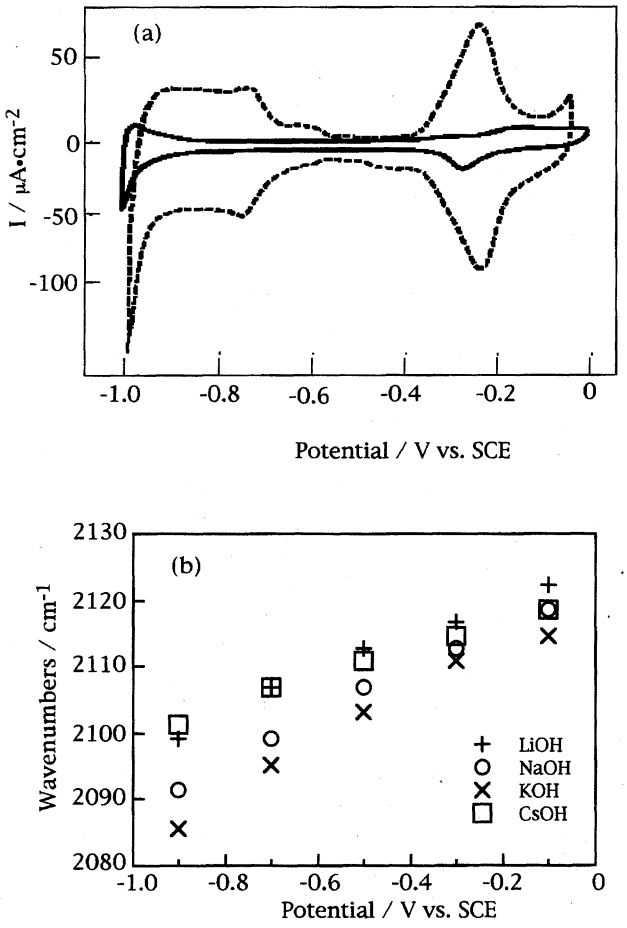

Fig. 6. (a): Cyclic voltammograms for Pt(111) electrode in 0.1 M NaOH. Solid line: CN-coated Pt(111). Dashed line: bare Pt(111). Scan rate=0.05 $V\,s^{-1}$. (b): Change in peak position of the C–N stretching vibration frequency of CN on Pt(111) in 0.1 M LiOH (+), NaOH (○), KOH (×), and CsOH (□). Background potentials were 0.6, 0.6, 0.8, and 0.7 V vs. SCE, for LiOH, NaOH, KOH, and CsOH, respectively.

ure 6(b) shows the potential dependence of the peak position of C–N vibrational stretching on Pt(111) in the alkaline solutions. In all solutions with extremely low concentrations of H_3O^+, no bending was observed in the peak-position curve. This result appears to suggest that there is no exchange of cation with H_3O^+. At cathodic potentials, the band frequency varies in the order $Cs^+ \approx Li^+ > Na^+ > K^+$ as can be seen in Fig. 6(b). On the other hand, at potentials more positive than −0.3 V, the peaks are located at almost the same frequency, indicating little influence of the nature of cations on the C–N vibration. The slope for the frequency shift is the highest in KOH solution (37 $cm^{-1}\,V^{-1}$). Na^+ gives the second highest slope (34 $cm^{-1}\,V^{-1}$) (Fig. 4), followed by Li^+ (23 $cm^{-1}\,V^{-1}$) and Cs^+ (19 $cm^{-1}\,V^{-1}$).

Rosasco et al.[20] examined the strength of interaction between cations and CN on Pt(111) by ex-situ measurements. The order of the interaction strength of some of the cations was reported to be $Mg^{2+} \gg K^+ > Na^+ = Cs^+ > H_3O^+ > Li^+$. They concluded that on the CN layer highly charged cations are retained most strongly, followed by cations of relatively small size and those least strongly hydrated. Ashley et al.[33] carried out IRAS measurements of the C–N stretching band of SCN adsorbed on a polycrystalline Pt electrode in 0.1 M $LiClO_4$, $NaClO_4$, $KClO_4$, and $CsClO_4$. They found that, at a cathodic potential below ca. −0.3 V vs. SCE, the band frequency for C–N stretching follows the order: $Li^+ > Cs^+ > K^+ > Na^+$. The cation effect was most pronounced at very negative potentials. It was reported that the magnitude of the electric field is dependent on the distance of the OHP from the electrode,[22] and the smaller distance gives the larger electrochemical Stark effect. In our experiments for CN adsorbed on Pt(111) in alkaline solutions, the influence of cations on CN is profound at cathodic potentials, where the OHP's for the cations are closer to the electrode surface, probably in the order $K^+ > Na^+ > Li^+ \approx Cs^+$ (Fig. 6(b)). At anodic potentials, the cations are located away from the electrode surface, thus giving only small differences between them.

IRAS Measurements in $HClO_4$ and in $Mg(ClO_4)_2$. The cation effects of H_3O^+ and Mg^{2+} on CN at Pt(111) were subsequently investigated by using IRAS. Figure 7(a) shows the CV's on bare (dashed line) and CN-modified Pt(111) (solid line) in 0.1 M $HClO_4$. In spite of the fact that the electrode surface was covered with CN, a broad pair of peaks appeared in the potential range more negative than 0.2 V. After subtracting the double layer charging current, a charge density of 73 $\mu C\,cm^{-2}$ was obtained for the reduction peak between −0.3 and 0.2 V, suggesting that hydrogen adsorption was not entirely blocked by the adsorption of CN in the acidic solution. The IRAS measurements were carried out in a $HClO_4$ solution, and as in the previous cases a single peak appeared at ca. 2100 cm^{-1} at potentials between −0.25 and 0.45 V. Figure 7(b) shows the potential dependency of the peak position of CN on Pt(111) in 0.1 M $HClO_4$. In the curve, a change in slope was observed at 0.15 V. At potentials more negative than 0.15 V, the slope for the frequency change was 82 $cm^{-1}\,V^{-1}$. On the other hand, the slope was extremely small, 11 $cm^{-1}\,V^{-1}$,

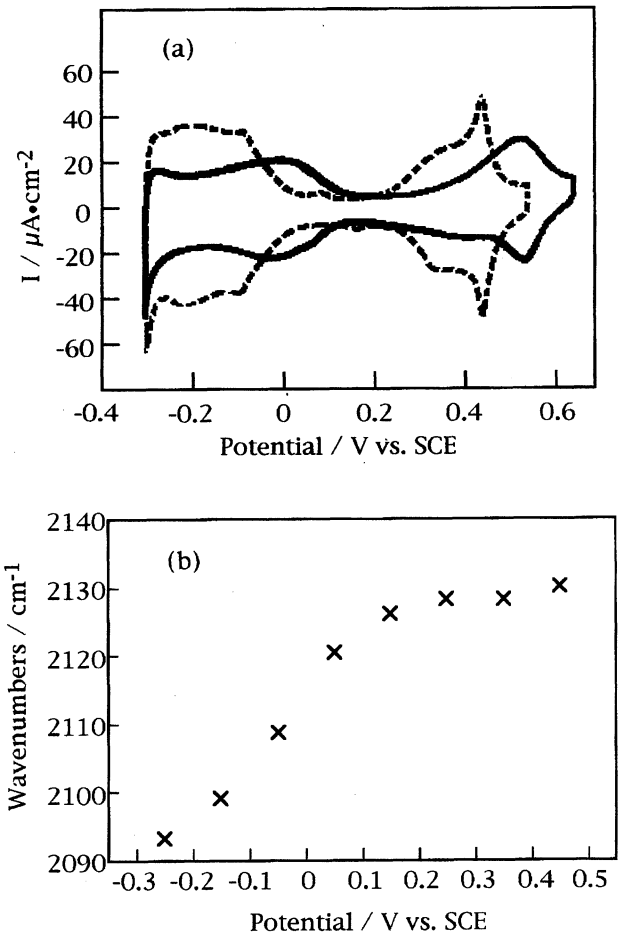

Fig. 7. (a): Cyclic voltammograms for Pt(111) electrode in 0.1 M $HClO_4$ (pH = 1). Solid line: CN-coated Pt(111). Dashed line: bare Pt(111). Scan rate= 0.05 $V\,s^{-1}$. (b): Change in peak position of the C–N stretching vibration frequency of CN on Pt(111) in 0.1 M $HClO_4$. Background potential = 1.15 V vs. SCE.

at potentials more anodic than 0.15 V. Ashley et al. argued that the differences induced in the potential field at the interface by variances in the electrode-OHP distance are not as sensitive at very positive potentials,[33] where the concentration of counter cation at the interface is also expected to be smaller. We believe that this mechanism applies similarly to H_3O^+ in this acidic solution. Notably, in-situ STM measurements have revealed a structural change also at 0.15 V.[12] As the potential is scanned more cathodic than 0.15 V, the $(2\sqrt{3}\times 2\sqrt{3})R30°$ is transformed to $(\sqrt{7}\times\sqrt{7})R19.1°$ with the change in coverage for CN from 0.58 to 0.57 (too subtle to be detectable by IRAS). Therefore, the change in CN structure on Pt(111) and the hydrogen adsorption–desorption (Fig. 7(a)) simultaneously take place at 0.15 V with the change in slope in the peak frequency–potential curve induced by the cation–OHP distance.

Finally, as an example of cations with multiple charges, we present IRAS in 0.1 M $Mg(ClO_4)_2$ (pH = 7). As Hubbard and coworkers have shown,[20] cations with multiple charges are adsorbed very strongly on the CN layer. Figure 8 shows

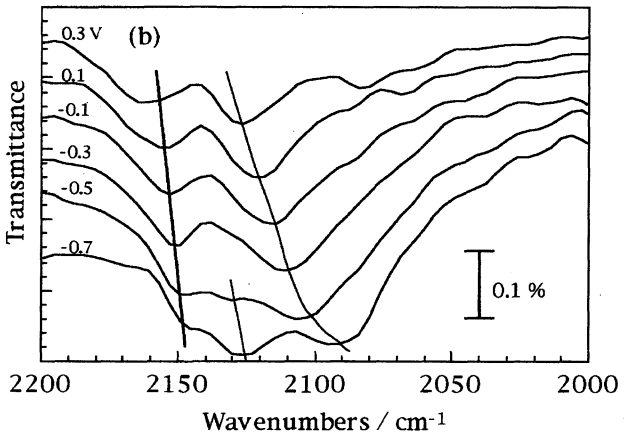

Fig. 8. Potential dependence of IR spectra of CN on Pt-(111) in a 0.1 M $Mg(ClO_4)_2$ solution. pH = 7. Background potential= 0.9 V vs. SCE.

the potential dependent spectra of CN on Pt(111) in $Mg(ClO_4)_2$. The spectra were completely different from those for any cation so far described. Although the peak near 2100 cm^{-1} was observed with other cations, two additional peaks were observed at ca. 2130 and 2150 cm^{-1}. Those newly-found peaks are also of surface species because their frequencies change with potential. The peak at ca. 2130 cm^{-1} disappeared as the potential was raised from −0.7 V to −0.3 V. The peak at ca. 2150 cm^{-1} shifted toward higher frequencies, but the rate was as small as 14 cm^{-1} V^{-1}. These peculiar behaviors cannot be explained by the simple electrochemical Stark effect. The existence of three types of peaks may indicate a multiple configuration of Mg^{2+} in OHP. This strong influence of Mg^{2+} could not be understood solely by IRAS. Other techniques such as STM and AFM may provide explanation for this effect.

Conclusions

To understand the effect of cations in OHP on CN in IHP, in-situ IRAS measurements were carried out in various electrolyte solutions for the C–N stretching mode using a CN-modified Pt(111) electrode surface. In solutions containing H_3O^+, Li^+, Na^+, K^+, and Cs^+ as electrolyte cations, only a single peak at ca. 2100 cm^{-1} was observed, and the peak frequency became lower as the potential was scanned in the cathodic direction. In a $KClO_4$ solution (pH = 9.5), a change in slope was observed at −0.5 V in the frequency-potential curve as the potential was scanned in the cathodic direction, implying that H_3O^+ dominates in OHP at cathodic potentials even in the solution of $KClO_4$. In highly alkaline solutions, the slope for the frequency shift is dependent on the cations, and the order was calculated as $K^+ > Na^+ > Li^+ > Cs^+$. In $HClO_4$, a change in slope was also observed in the frequency–potential curve. In a $Mg(ClO_4)_2$ solution, three peaks are observed for the CN on Pt(111), possibly due to a multiple configuration of Mg^{2+} in OHP.

This work was supported by Ministry of Education, Science, Sports, and Culture, Grant-in-Aid for Research No. 07215209 and 07855097, ERATO-Itaya Electrochemiscopy Project, JRDC, and partly by Foundation Advanced Technology Institute. The authors thank Dr. Y. Okinaka for his help in the writing of this manuscript.

References

1) P. Delahay, "Double Layer and Electrode Kinetics," Interscience Publications, London (1965).
2) K. Ashley and S. Pons, *Chem. Rev.*, **88**, 673 (1988).
3) H. Siegenthaler, in "Scanning Tunneling Microscopy II," ed by R. Wiesendanger and H.-J. Güntherrodt, Springer-Verlag, Berlin (1992), p. 7.
4) P. A. Cristensen, *Chem. Soc. Rev.*, **1992**, 197.
5) B. M. Ocko, G. M. Watson, and J. Wang, *J. Phys. Chem.*, **98**, 897 (1994).
6) S.-L. Yau, C. M. Virtus, and B. C. Schardt, *J. Am. Chem. Soc.*, **112**, 3677 (1990).
7) X. Gao and M. J. Weaver, *J. Am. Chem. Soc.*, **144**, 8544 (1992).
8) S. Sugita, T. Abe, and K. Itaya, *J. Phys. Chem.*, **97**, 8780 (1993).
9) T. Yamada, N. Batina, and K. Itaya, *J. Phys. Chem.*, **99**, 8817 (1995).
10) S. Tanaka, S.-L. Yau, and K. Itaya, *J. Electroanal. Chem.*, **396**, 125 (1995).
11) C. Stuhlmann, L. Villegas, and M. J. Weaver, *Chem. Phys. Lett.*, **219**, 339 (1994).
12) Y.-G. Kim, S.-L. Yau, and K. Itaya, *J. Am. Chem. Soc.*, **118**, 393 (1996).
13) O. M. Magnussen, J. Hagebock, J. Hotlos, and R. J. Behm, *Faraday Discuss. Chem. Soc.*, **94**, 329 (1992).
14) G. J. Edens, X. Gao, and M. J. Weaver, *J. Electroanal. Chem.*, **375**, 357 (1994).
15) A. M. Funtikov, U. Linke, U. Stimming, and R. Vogel, *Surf. Sci.*, **327**, L343 (1995).
16) L.-J. Wan, S.-L. Yau, and K. Itaya, *J. Phys. Chem.*, **99**, 9507 (1995).
17) J. Inukai, S. Sugita, and K. Itaya, *J. Electroanal. Chem.*, **403**, 159 (1996).
18) R. Parsons, in "Modern Aspects of Electrochemistry," ed by J. O'M. Bockris and B. E. Conway, Butterworths Scientific Publications, London (1954), p. 103.
19) J. L. Stickney, S. D. Rosasco, G. N. Salaita, and A. T. Hubbard, *Langmuir*, **1**, 66 (1985).
20) S. D. Rosasco, J. L. Stickney, G. N. Salaita, D. G. Frank, J. Y. Katekaru, B. C. Schardt, M. P. Soriaga, D. A. Stern, and A. T. Hubbard, *J. Electroanal. Chem.*, **188**, 95 (1985).
21) D. G. Frank, J. Y. Katekaru, S. D. Rosasco, G. N. Salaita, B. C. Schardt, M. P. Soriaga, D. A. Stern, J. L. Stickney, and A. T. Hubbard, *Langmuir*, **1**, 587 (1985).
22) J. O'M. Bockris and A. K. N. Reddy, "Modern Electrochemistry," Plenum Press, New York (1973), Vol. 2.
23) N. K. Ray and A. B. Anderson, *Surf. Sci.*, **125**, 803 (1983).
24) F. Kitamura, M. Takahashi, and M. Ito, *Surf. Sci.*, **223**, 493 (1989).
25) K. Sashikata, N. Furuya, and K. Itaya, *J. Electroanal. Chem.*, **336**, 361 (1991).
26) H. Seki, K. Kunimatsu, and W. G. Gorden, *Appl. Spectros.*, **39**, 437 (1985).
27) C. S. Kim and C. Korzeniewski, *J. Phys. Chem.*, **97**, 9784

(1993).
28) F. Kitamura, M. Takahashi, and M. Ito, *Chem. Phys. Lett.*, **130**, 181 (1986).
29) F. T. Wanger and R. N. Ross, *J. Electroanal. Chem.*, **250**, 301 (1988).
30) E. Morallon, J. Vazquez, and A. Aldaz, *J. Electroanal. Chem.*, **334**, (1992).
31) J. K. Foley, S. Pons, and J. J. Smith, *Langmuir*, **1**, 697 (1985).
32) D. S. Corrigan and M. J. Weaver, *J. Phys. Chem.*, **90**, 5300 (1986).
33) K. Ashley, M. G. Samant, H. Seki, and M. R. Philipott, *J. Electroanal. Chem.*, **270**, 349 (1989).